

Defect-engineered blue-violet electroluminescence from Ge nanocrystal rich SiO₂ layers by Er doping

A. Kanjilal, L. Rebohle, M. Voelskow, W. Skorupa, and M. Helm

Citation: *Journal of Applied Physics* **106**, 026104 (2009); doi: 10.1063/1.3183904

View online: <http://dx.doi.org/10.1063/1.3183904>

View Table of Contents: <http://scitation.aip.org/content/aip/journal/jap/106/2?ver=pdfcov>

Published by the [AIP Publishing](#)

Articles you may be interested in

Controlling blue-violet electroluminescence of Ge-rich Er-doped SiO₂ layers by millisecond annealing using flash lamps

J. Appl. Phys. **107**, 023114 (2010); 10.1063/1.3296252

Electroluminescence induced by Ge nanocrystals obtained by hot ion implantation into SiO₂

J. Appl. Phys. **106**, 106103 (2009); 10.1063/1.3262627

The role of Ge-related oxygen-deficiency centers in controlling the blue-violet photo- and electroluminescence in Ge-rich SiO₂ via Er doping

J. Appl. Phys. **106**, 063112 (2009); 10.1063/1.3225911

Enhanced blue-violet emission by inverse energy transfer to the Ge-related oxygen deficiency centers via Er³⁺ ions in metal-oxide semiconductor structures

Appl. Phys. Lett. **94**, 051903 (2009); 10.1063/1.3077169

Light emission and charge trapping in Er-doped silicon dioxide films containing silicon nanocrystals

Appl. Phys. Lett. **86**, 151914 (2005); 10.1063/1.1872208



Not all AFMs are created equal
Asylum Research Cypher™ AFMs
There's no other AFM like Cypher

www.AsylumResearch.com/NoOtherAFMLikeIt

OXFORD
INSTRUMENTS
The Business of Science®

Defect-engineered blue-violet electroluminescence from Ge nanocrystal rich SiO₂ layers by Er doping

A. Kanjilal,^{a)} L. Rebohle, M. Voelskow, W. Skorupa, and M. Helm

Institute of Ion Beam Physics and Materials Research, Forschungszentrum Rossendorf, P.O. Box 51 01 19, 01314 Dresden, Germany

(Received 6 April 2009; accepted 24 June 2009; published online 29 July 2009)

Using combined microstructural and electroluminescence (EL) investigations of the Er-doped Ge-rich SiO₂ layers, it is established that the Ge-related oxygen-deficiency centers (GeODCs), which are associated with the 407 nm light emission, are situated at the Ge nanocrystal/SiO₂ interface. Electrically driven energy transfer from the Er³⁺ to GeODCs causes an increase in the 407 nm EL intensity. It reaches a maximum before quenching with increasing Er concentration due to the crystalline-to-amorphous transition of Ge nanocrystals. Ge concentration dependent quenching of the maximum EL intensity and the peak shifting toward higher Er concentration are discussed in terms of the reduction of the surface-to-volume ratio with increasing nanocrystal size. © 2009 American Institute of Physics. [DOI: [10.1063/1.3183904](https://doi.org/10.1063/1.3183904)]

Doping of Er in Ge nanocrystal (NC) rich metal-oxide-semiconductor (MOS) structures and its impact on the electroluminescence (EL) properties have recently been demonstrated.¹ The Er-ions in such electrically driven systems were shown to act like *sensitizers* in pumping the adjacent Ge-related oxygen deficiency centers (GeODCs), leading to an increase in intensity of the blue-violet EL at the expense of the 1.53 μm Er emission. This phenomenon is in contrary to the well-known energy transfer mechanism from optically excited semiconductor nanoparticles, especially Si NCs to the nearest Er³⁺ ions^{2–4} and thus termed as inverse energy transfer (IET) process.¹ Although the prototype we consider has shown an opposite mechanism during electrical pumping in practice,¹ the complete knowledge of the Er dose dependent damage production in Ge-rich SiO₂ has not yet been explored. Ion beam induced amorphization of NCs has been reported for Si NCs,⁵ and more recently for Ge NCs.⁶ In fact, the photoluminescence intensity was shown to quench with increasing ion dose due to the enhancement of the mean number of damaged Si NCs.⁵ Naturally the Ge-rich SiO₂ can serve as a model system for studying the defect properties, since the electrically active GeODCs often play a more important role than Ge NCs.

In this communication, we report the correlation between the microstructure and the EL properties of Ge-rich SiO₂ with increasing Er-doping concentration (C_{Er}). In particular, a deterioration of the microstructure, especially the reduction in the effective fraction of crystalline Ge grains, will be addressed with increasing C_{Er} for a fixed volume of Ge NCs and shown to be responsible for the EL quenching beyond a critical C_{Er} due to the loss of GeODCs.

The standard MOS structure was fabricated by local oxidation of Si (LOCOS) technology with a 200 nm thick thermally grown SiO₂ layer on *n*-type Si(100) wafer. Initially 130 keV Ge ions were implanted at room temperature (RT) with a dose of $2\text{--}6 \times 10^{16}$ ions/cm², corresponding to the

maximum Ge concentration lying in between 3.5% and 11.1% at R_p as derived from the SRIM-2006 calculations.⁷ The samples were subjected to furnace annealing for 60 min at 950 °C to produce Ge NCs. Subsequently, 250 keV Er ions were implanted with a dose of $1\text{--}5 \times 10^{15}$ ions/cm² (i.e., 0.3%–1.4% Er at R_p) followed by annealing at 900 °C for 30 min to remove implantation-induced defects and for activating Er³⁺ ions.⁸ The Ge and Er concentrations were further verified by Rutherford backscattering spectrometry (RBS) measurements. A 100 nm thick silicon-oxynitride layer was deposited on top of the LOCOS structure. Moreover, semitransparent indium-tin oxide (ITO) and aluminum contacts were sputter deposited on the front and rear surfaces, respectively. The top layer was further patterned by optical lithography to achieve arrays of circular electrodes (diameter ~ 300 μm). Transmission-electron-microscopy (TEM) images were taken by a FEI Titan 80–300 S/TEM instrument under cross-sectional geometry. All the RT EL spectra were recorded with constant current mode and under forward bias conditions, and by a monochromator in combination with a photomultiplier or liquid nitrogen cooled In-GaAs detector. The photomultiplier in combination with a photocounting system was used to study the time-resolved EL dynamics.

Considering the EL spectrum of the only Er-doped SiO₂,⁹ the enhanced 407 nm EL intensity from the Ge-rich SiO₂ layers for a current density (J) of 1.4 mA/cm² in presence of Er [Fig. 1(a)] can be explained in terms of the IET process; see Ref. 1 for details. Figure 1(b) summarizes the C_{Er} dependence of the 407 nm EL peak intensity (I) normalized to the maximum peak intensity (I_{max}) for each of the three Ge concentrations (C_{Ge}) of 3.5%, 7.4%, and 11.1%. In fact, the maximum EL intensity seems to decrease almost linearly with increasing C_{Ge} , while the peak position shifts toward higher C_{Er} [Fig. 1(c)]. Similarly, the variation of the 1535 nm Er EL intensity normalized to the maximum peak intensity at 1.4% Er is displayed in Fig. 1(d). Clearly, the maximum EL intensity drops by more than an order of mag-

^{a)}Electronic mail: a.kanjilal@fzd.de.

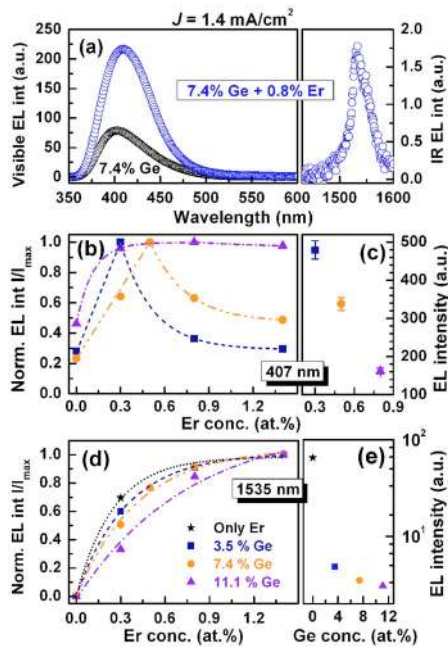


FIG. 1. (Color online) The EL spectra of the Ge-rich MOS structures in presence (0.8%) and absence of Er for $J=1.4$ mA/cm² (a). The variation of the normalized 407 nm EL intensity with increasing C_{Er} is shown in (b), while the change of the maximum 407 nm EL intensity is plotted in (c). The variation of the normalized 1535 nm EL intensity (d) and the maximum of the 1535 nm EL intensity (e) for only Er-doped MOS structures, which were heat treated by only second annealing condition allow to follow the change in EL intensity in presence of excess Ge.

nitude in presence of excess Ge [Fig. 1(e)], demonstrating that most of the optically active Er^{3+} ions (more than 90%) are involved in the IET process.¹ Careful observation reveals that each normalized 407 nm EL intensity profile [Fig. 1(b)] shows a similar tendency that consists of an initial increase in EL intensity, followed by a quenching at higher C_{Er} . Conversely, an exponential increase in intensity is noticed for each normalized 1535 nm EL profile [Fig. 1(d)]. Moreover, no significant change in 407 nm EL decay time (τ_d) was noticed for a fixed C_{Ge} with increasing C_{Er} , suggesting that (i) Er does not add an additional nonradiative decay path and (ii) no energy transfer from Ge NC to the Er^{3+} ions has occurred.⁴ However, the τ_d is decreased from 65.9 μ s (for 3.5% Ge) to 62.1 and 48.2 μ s for 7.4% and 11.1% Ge, respectively, indicating that a nonradiative decay path is introduced with increasing C_{Ge} .

For understanding the detailed mechanism behind the observed EL properties, it is essential to follow the microstructural evolution in the corresponding oxide layers. The formation of Ge NCs in only Ge-rich SiO_2 layers has been verified initially by high-resolution TEM (HRTEM), keeping the electron beam direction along [011]-zone axis. The growth of Ge NCs can be discussed in the framework of depth dependent local degree of Ge saturation, while the average crystallite size was found to increase with increasing C_{Ge} . For instance, the Ge NC size was determined to be ~ 6.1 , 9.4, and 13.6 nm for 3.5%, 7.4%, and 11.1% Ge, respectively. Moreover, a gradual modification of Ge NCs has been observed with increasing C_{Er} . We have chosen here exemplarily a particular C_{Ge} , namely, 3.5% Ge to follow the

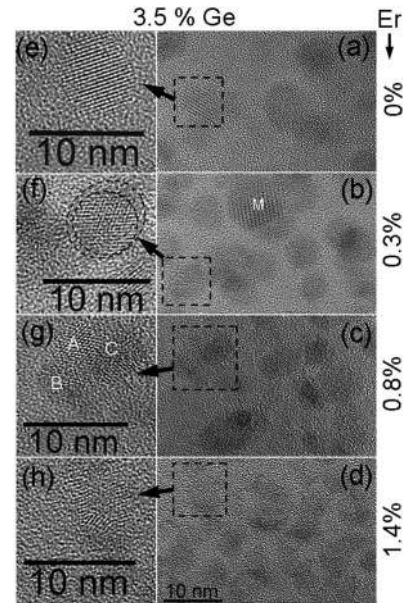


FIG. 2. Cross-sectional TEM images of the only Ge-rich SiO_2 (a) and the Er-doped Ge-rich SiO_2 with concentrations of 0.3% (b), 0.8% (c), and 1.4% (d) Er for 3.5% Ge. The corresponding HRTEM images are shown in (e) and (f), showing gradual reduction of the average NCs size from $\sim 6.1 \pm 2$ nm (a), $\sim 5.9 \pm 2$ nm (b), $\sim 3.5 \pm 2$ nm (c), and $\sim 2.7 \pm 1$ nm (d), respectively.

ongoing changes in microstructure with increasing Er dose [Figs. 2(a)–2(d)].

As apparent from Fig. 2(a), the spherical Ge NCs are randomly oriented; the HRTEM image of an {111}-faceted NC is displayed in Fig. 2(e). Indeed, a fraction ($\sim 10\%$) of Ge was diffused toward the Si/ SiO_2 interface during annealing as revealed from RBS. Following the low dose Er implantation (0.3%), hardly any change was observed in the overall microstructure [Fig. 2(b)]. However, close inspection of a NC reveals the formation of a shell-like structure with a thin amorphous layer (light-gray contrast) at the NC/ SiO_2 interface; this is indicated by dashed circles in Fig. 2(f). Although the observed feature resembles Er-doped Si NCs (Ref. 10), ion beam induced preferential amorphization of Ge NCs has also been invoked in Ref. 6. To evaluate the configuration of this amorphous feature [Fig. 2(f)], we correlate the corresponding EL results, as addressed in the following. Moreover, the average size of Ge NCs was found to decrease gradually from $\sim 6.1 \pm 2$ to 2.7 ± 1 nm with increasing Er concentration from 0% to 1.4%, respectively. Although a few bigger Ge NCs with diameter of ~ 10 nm were observed even after 0.3% Er doping [marked by “M” in Fig. 2(b)], no such big NCs were detected in case of 0.8% and 1.4% Er.

With increasing Er dose up to 0.8%, a large number of fragmented and partially amorphized crystalline Ge clusters were observed [Figs. 2(c)]. Since the second annealing was carried out at 900 °C, which is lower than that of the melting temperature of Ge NCs,¹¹ it is unlikely to have an amorphous-to-crystalline transition of the damaged Ge clusters. The corresponding HRTEM image [Figs. 2(g)] depicts three distinct regions, indicated by “A” (crystalline), “B” (amorphous in light-gray), and “C” (amorphous in dark-gray). In fact, the observed change in contrast in B and C can

be classified in view of the formation of a variety of non-crystalline Er composites, which depend strongly on the ratio of Er and O atoms and the interaction strength in Ge-rich environment.¹² The formation of Er oxide clusters is also possible.⁹ Indeed, the Er-ion beam induced damage becomes more pronounced at 1.4% Er [Fig. 2(d)] where the HRTEM image of a severely damaged NC is projected in Fig. 2(h). In a similar fashion, the crystalline-to-amorphous phase transition has also been observed for 7.4% Ge where the NC degradation starts from 0.5% Er (not shown).

By correlating the microscopic observations with the EL results, it is evident that the 407 nm EL quenching [Fig. 1(b)] is associated with the crystalline-to-amorphous transition or fragmentation of Ge NCs (Fig. 2). In fact, the parallel increase in the normalized 1535 nm EL intensity [Fig. 1(d)] implies that the higher lying states of Er^{3+} ions are now populating the $^4I_{13/2}$ state instead of transferring the energy to GeODCs. Such phenomena can arise if more and more Er ions try to coalesce and form thermodynamically stable Er oxide clusters like in Ref. 9 due to the gradual loss of the GeODCs as a function of Er-ion dose. Er concentration dependent loss of effective GeODCs has also been confirmed by performing photoluminescence (PL) investigations using a 266 nm wavelength¹³—nonresonant to the Er^{3+} levels,¹⁴ showing a continuous quenching of the blue-violet PL intensity with increasing Er doping without any change in PL decay times. Since the existence of GeODCs is strongly related with the quality of Ge NCs, we can conclude that most of the EL-active GeODCs are preferably situated at the NC/ SiO_2 interface. Indeed, the Er^{3+} ions residing at the surface of the Er oxide clusters can either take part in energy transfer process to the remaining GeODCs and/or emit light as usual.⁹ Interestingly, the maximum EL efficiency [Fig. 1(c)] and the shell-like structure [Fig. 2(f)] are observed at the initial stage of Er doping (0.3%) for 3.5% Ge. Bearing in mind the requirement of the Er^{3+} ions in the vicinity of the GeODCs for accomplishing an IET process,¹ the formation of an Er-rich oxide layer at the NC/ SiO_2 interface is more probable, creating a shield for separating the Ge core from the surrounding SiO_2 matrix. However, a fraction of interfacial Er oxide may undergo a phase transition to form stable Er complexes via ion-beam mixing. This effect will be more severe and accompanied by the amorphization and fragmentation of the Ge NCs with further increase in Er-ion dose (schematically exhibited in Fig. 3). Moreover, the Debye-Waller factor is known to increase with decreasing surface-to-volume ratio¹⁵ and therefore, a relatively low dose is sufficient for a crystalline-to-amorphous transition of smaller NCs.⁶ Due to low statistics in Fig. 1(b), it is impossible to discuss the observed 407 nm EL quenching quantitatively. Clearly, the decrease in EL intensity is associated with the quenching of the IET process due to the fragmentation and amorphization of Ge NCs, whereas Fig. 1(c) reveals that the probability of the Er^{3+} -GeODC interaction is reduced significantly with decreasing surface-to-volume ratio of the NC.

In summary, combining the TEM and EL results we demonstrate that the GeODCs responsible for the 407 nm light emission reside at the Ge NC/ SiO_2 interface. Electric-

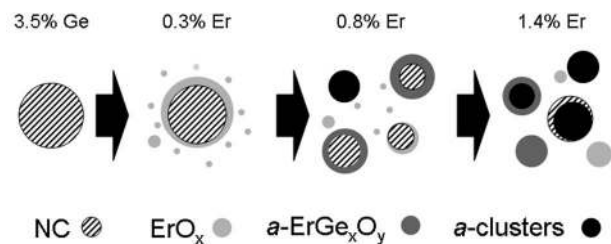


FIG. 3. Schematic representation of the Er-dose dependent microstructural modification of the Ge NC embedded SiO_2 layer: a NC will first transform to a shell-like structure by 0.3% Er doping. For 0.8% Er, part of the NC is transformed to ErGe_xO_y , partially fragmented and partially amorphous (marked as *a*) clusters. With 1.4% Er, fragmented NCs are mostly transformed to amorphous clusters and ErGe_xO_y complexes.

cally driven energy transfer from the Er^{3+} to the GeODCs can be maximized when an Er oxide layer is formed around a NC—giving the highest 407 nm EL intensity. Beyond a critical Er concentration, the 407 nm EL quenching is explained in terms of the fragmentation and amorphization of Ge NCs in conjunction with the ion-beam mixing enhanced formation of stable Er complexes. Moreover, Ge concentration-dependent quenching of the maximum EL intensity with a shift in this maximum toward higher Er concentration is discussed in the light of a decrease in the surface-to-volume ratio with increasing NC size.

Authors thank the Rossendorf Implantation Group for ion implantation and H. Felsmann, C. Neisser, and G. Schnabel for their careful semiconductor preparation work. The support of the Alexander von Humboldt Foundation is gratefully acknowledged.

- ¹A. Kanjilal, L. Rebohle, M. Voelskow, W. Skorupa, and M. Helm, *Appl. Phys. Lett.* **94**, 051903 (2009).
- ²M. Fujii, M. Yoshida, Y. Kanzawa, S. Hayashi, and K. Yamamoto, *Appl. Phys. Lett.* **71**, 1198 (1997).
- ³B. Garrido, C. García, S.-Y. Seo, P. Pellegrino, D. Navarro-Urrios, N. Daldosso, L. Pavesi, F. Gourbilleau, and R. Rizk, *Phys. Rev. B* **76**, 245308 (2007).
- ⁴A. Kanjilal, L. Rebohle, M. Voelskow, W. Skorupa, and M. Helm, *J. Appl. Phys.* **104**, 103522 (2008).
- ⁵D. Pacifici, E. C. Moreira, G. Franzò, V. Martorino, F. Priolo, and F. Iacona, *Phys. Rev. B* **65**, 144109 (2002).
- ⁶M. C. Ridgway, G. de M. Azevedo, R. G. Elliman, C. J. Glover, D. J. Llewellyn, R. Miller, W. Wesch, G. J. Foran, J. Hansen, and A. Nylandsted-Larsen, *Phys. Rev. B* **71**, 094107 (2005).
- ⁷J. F. Ziegler and J. P. Biersack, SRIM-2006.02 (<http://www.srim.org>).
- ⁸A. Janotta, M. Schmidt, R. Janssen, M. Stutzmann, and Ch. Buchal, *Phys. Rev. B* **68**, 165207 (2003).
- ⁹A. Kanjilal, L. Rebohle, W. Skorupa, and M. Helm, *Appl. Phys. Lett.* **94**, 101916 (2009).
- ¹⁰P. Pellegrino, B. Garrido, J. Arbiol, C. Garcia, Y. Labour, and J. R. Morante, *Appl. Phys. Lett.* **88**, 121915 (2006).
- ¹¹Q. Xu, I. D. Sharp, C. W. Yuan, D. O. Yi, C. Y. Liao, A. M. Glaeser, A. M. Minor, J. W. Beeman, M. C. Ridgway, P. Kluth, J. W. Ager III, D. C. Chrzan, and E. E. Haller, *Phys. Rev. Lett.* **97**, 155701 (2006).
- ¹²A. Kanjilal, L. Rebohle, N. K. Baddela, S. Zhou, M. Voelskow, W. Skorupa, and M. Helm, *Phys. Rev. B* **79**, 161302(R) (2009).
- ¹³A. Kanjilal, S. Tsushima, C. Götz, L. Rebohle, M. Voelskow, W. Skorupa, and M. Helm (unpublished).
- ¹⁴G. H. Dieke, *Spectra and Energy Levels of Rare Earth Ions in Crystals* (Interscience, New York, 1968), Chap. 13.
- ¹⁵L. L. Araujo, R. Giulian, D. J. Sprouster, C. S. Schnohr, D. J. Llewellyn, P. Kluth, D. J. Cookson, G. J. Foran, and M. C. Ridgway, *Phys. Rev. B* **78**, 094112 (2008).